metals

MDPI

Article

Microstructure and Mechanical Properties of Cast and Hot-Rolled Medium-Carbon Steels under Isothermal Heat-Treatment Conditions

Byungsue Shin [1], Kwangyuk Kim [1], Sung Yi [2], Sanggyu Choi [1] and Soongkeun Hyun [1,*]

[1] Department of Materials Science and Engineering, Inha University, Incheon 22212, Korea; 22202189@inha.edu (B.S.); kky1216@inha.ac.kr (K.K.); sanggyuchoi@inha.edu (S.C.)
[2] Department of Mechanical and Materials Engineering, Portland State University, Portland, OR 97207-0751, USA; syi@pdx.edu
* Correspondence: skhyun@inha.ac.kr; Tel.: +82-32-850-0215

Abstract: In this study, the changes in the microstructure and mechanical properties during isothermal heat treatment of cast steel before and after hot deformation were investigated using medium-carbon steel with low alloy content. The microstructural characteristics of the cast and hot-rolled medium-carbon steel under isothermal heat-treatment conditions were examined using optical microscopy and scanning electron microscopy in conjunction with electron backscatter diffraction. The variation in the mechanical properties was evaluated using Rockwell hardness and tensile tests. After maintaining an austenitizing condition at 1200 °C for 30 min, an isothermal heat treatment was performed in the range 350–500 °C, followed by rapid cooling with water. Both the cast steel and hot-rolled steel did not completely transform into bainitic ferrite during isothermal heat treatment. The partially untransformed microstructure was a mixture of martensite and acicular ferrite. At 500 °C, the prior austenite phase changed to Widmanstätten ferrite and pearlite. At 450 °C, bainitic ferrite and cementite were coarsened by the coalescence of ferrite and subsequent diffusive growth. The mechanical properties increased as the isothermal heat-treatment temperature decreased, and the hardness of the cast steel was generally higher than that of the hot-rolled steel. Hardness and strength showed similar trends, and overall mechanical properties tend to decrease as the isothermal heat-treatment temperature increases, but there are slight differences depending on complex factors such as various phase fractions and grain size.

Keywords: medium-carbon low-alloy steel; isothermal heat treatment; phase fraction; bainite; degenerated upper bainite; bainitic ferrite; multiphase steel

check for updates

Citation: Shin, B.; Kim, K.; Yi, S.; Choi, S.; Hyun, S. Microstructure and Mechanical Properties of Cast and Hot-Rolled Medium-Carbon Steels under Isothermal Heat-Treatment Conditions. *Metals* **2021**, *11*, 1950. https://doi.org/10.3390/met11121950

Academic Editor: Lucia Morales-Rivas

Received: 27 October 2021
Accepted: 30 November 2021
Published: 3 December 2021

Publisher's Note: MDPI stays neutral with regard to jurisdictional claims in published maps and institutional affiliations.

Copyright: © 2021 by the authors. Licensee MDPI, Basel, Switzerland. This article is an open access article distributed under the terms and conditions of the Creative Commons Attribution (CC BY) license (https://creativecommons.org/licenses/by/4.0/).

1. Introduction

In general, steel needs to be of high strength with a light weight for automobiles and with durability for civil engineering applications, machinery, and building structures. In particular, in the era of carbon neutrality, the features of materials have become more critical to their applications. Bainitic steels are typically used in applications that require high strength and wear resistance combined with good toughness. When choosing the optimal material for a particular component, geometric constraints and desired properties are the determining factors. Alloys should have features such as the desired hardenability, economic feasibility, and resistance to unwanted phase formation, which can lead to poor mechanical properties or thermal cracking [1].

The entire scope and mechanisms of bainite formation and the structures controlling its mechanical properties are not fully understood. Several studies have been conducted on the contribution of various bainite microstructures to the mechanical properties [2–7].

Next-generation steels require both high strength and toughness along with microstructural control; that is, phase partitioning between martensite and bainitic ferrite. In

general, steels with a bainitic structure are controllable by limiting the carbon content up to 1.0 wt% by lowering the Ms transformation temperature [8].

Considering that high carbon content typically increases the deformation time and reduces weldability and impact toughness, the optimum carbon content in bainitic steel is a critical issue [9]. Because bainite formation [10] is a function of the transformation temperature, it is thought to play an important role in controlling the mechanical properties of steel. Tomita et al. [11,12] reported that lower bainite, which appears as needles and splits the prior austenite grains, has excellent mechanical properties, while upper bainite, which appears as a lump filling the prior austenite grains, has poor mechanical properties. Rao et al. [13] found that the impact toughness of high-strength low-alloy steels with a mixed microstructure of upper bainite and martensite was clearly increased without a reduction in strength.

Nevertheless, the increasingly poor use environment of steel requires improvement of the surface performance. In general, induction hardening, carburizing heat treatment, and nitriding heat treatment are applied to improve surface mechanical properties. Such surface treatment is good for abrasion resistance by increasing the hardness and strength of the surface. However, low elongation is not good for impact strength and the lifetimes are rather reduced. If the surface is applied plastic processing, the elongation and impact strength of the surface can be improved. Even low deformation at the surface has various effects on the internal microstructure and mechanical properties. Therefore, we are interested in the change in microstructure and mechanical properties not only in cast steel but also in a state with low deformation.

The current study evaluated the mechanical properties of medium-carbon low-alloy steel with respect to microstructure under low deformation and cast steels. Whereas conventional alloy steel is used for rolled and forged parts, cast steel is used in construction machinery and the mining industries. The relationship between the microstructure of the bainitic ferrite phase and the mechanical properties combined with various phase changes under isothermal heat treatment were investigated.

2. Materials and Methods

Table 1 shows the chemical composition of the medium-carbon low-alloy steel used in this study. The low-alloy steel was melted using a high-frequency induction melting furnace with a capacity of 10 kg. To remove impurities, a coagulant was used, and a small amount of Al was added to control the oxides. The ingot fabricated by Y-block sand casting was cut in half, one part was hot rolled, and the rest was heat treated. The reheating temperature of hot rolling was 1000 °C and the rolling temperature was 750 °C. A total of 3 passes were rolled, the thickness was 8 mm, and the reduction ratio was 30%. The size of the specimen is 20 mm × 125 mm × 12T for cast steel and 25 mm × 150 mm × 8T for hot-rolled steel.

Table 1. Chemical composition of the alloy steel (wt%).

C	Si	Mn	P	S	Cr	Ni	Cu	Al	Mo	Ti	V	Nb
0.314	0.539	1.321	0.019	0.011	0.515	0.252	0.084	0.028	0.028	0.002	0.006	0.015

The prepared samples were homogenized at 1200 °C for 4 h and quenched in water. To measure the variation in sample temperature during the heat treatment, a K-type thermocouple was spot welded to the center of the sample and connected to a recorder (GR-3500, Keyence, Osaka, Japan). The sample was heat treated under austenitizing conditions (1200 °C for 30 min) and then transferred directly to a salt bath for further isothermal heat treatment at 350–500 °C for 240 min. Nitrate was used as the salt in the salt bath, and after heat treatment, the sample was quenched in water. The isothermal heat-treatment process is illustrated in Figure 1. In the longitudinal direction of the isothermally heat-treated sample, 35 mm was used for microstructural analysis and surface hardness measurements, while the remaining 90 mm was used for tensile tests.

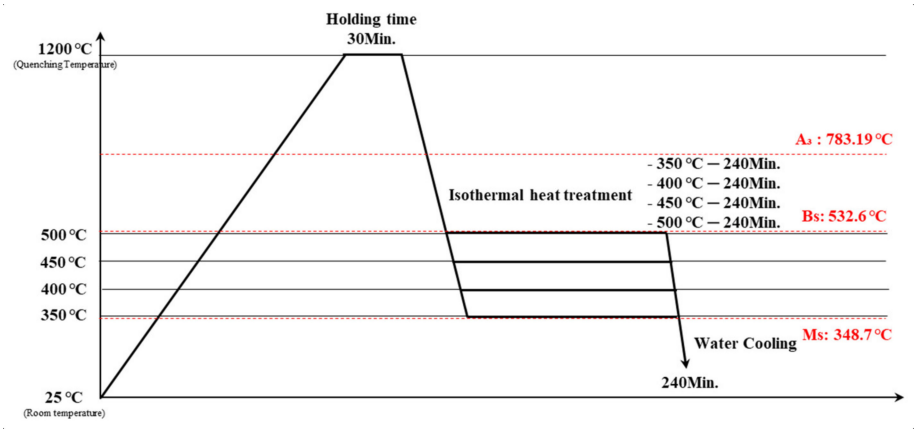


Figure 1. Schematic of the isothermal heat-treatment process.

Time-temperature-transformation (TTT) and continuous-cooling-transformation (CCT) diagrams were calculated using JMatPro software (Ver. 7) for detailed analysis of microstructural development after the various isothermal heat treatments. The samples for microstructural investigation were mechanically ground with sandpaper from #400 to #2000 and finally polished with 1 μm diamond paste. To reveal the microstructure, the samples were etched in 4% Picral (picric acid + ethanol) and LePera ($Na_2S_2O_5$ + DI water + picric acid + ethanol) etchants. The microstructure was investigated using optical microscopy (VHX-7000, Keyence, Osaka, Japan) and field-emission scanning electron microscopy (FE-SEM; SU5000, Hitachi, Japan). Electron backscatter diffraction (EBSD) analysis was performed to analyze the complex-shaped bainite-based microstructure. The EBSD specimens were mechanically polished and then electropolished using a spray-type electropolishing machine with 92% acetic acid and 8% perchloric acid. For performing EBSD analysis, the field-emission scanning electron microscope was used at an accelerating voltage, focal length, and step size of 30 kV, 10 mm, and 1.0 μm, respectively. EBSD analysis was performed in a FE-SEM and crystal orientation analysis was performed by EDAX (Ametek, PA, USA) in which orientation imaging microscopy (OIM) software was used. The phase fraction for each microstructure was measured by using Image-J software. The tensile tests were conducted using a universal testing machine (UTM; AGS-X, Shimadzu, Kyoto, Japan), for which the sample was prepared based on the ASTM E8M standard. The hardness was measured using a Rockwell hardness tester (RMT-3, Matuszawa, Akita, Japan) after mechanical grinding.

3. Results and Discussion

3.1. Microstructure

The CCT diagram shown in Figure 2 exhibits a C shape in the bainite region, with the "nose" at approximately 450 °C. A3 and Ms temperatures were adopted from the calculated JmatPro. Bs was formulated as follows [14]

$$\text{Bs } (^\circ\text{C}) = 656 - 57.7\text{C} - 35\text{Mn} - 75\text{Si} - 15.3\text{Ni} - 34\text{Cr} - 41.2\text{Mo [wt\%]} \quad (1)$$

The calculated Bs value is 532.56 °C, which is reasonable based on the TTT diagram. Below Bs, the austenite phase transforms into either bainitic ferrite or acicular ferrite. Above Bs, the austenite phase decomposes into pearlite through a diffusion mechanism. Consequently, polygonal ferrite is not expected to form under these isothermal heat-treatment conditions (350–500 °C), but bainite may form.

Reports for the past 20 years are microstructure classification methods according to the shape of ferrite, and different researchers use different microstructure nomenclature. Bramfitt and Speer [15] divided the microstructure that can be transformed from austenite into polygonal ferrite, pearlite, bainite, and martensite. B1-, B2-, B3-type bainite was subdivided and reported according to the type and shape. In addition, ISIJ Bainite Research

Group [16] analyzed and reported the ferrite and low-temperature transformation structures observed after continuous cooling treatment of ultra-low carbon steel with a chemical composition of 0.004C-0.62Si-0.71Mn-0.078Ti (wt%). According to their research results, ferrtie was classified into polygonal ferrite, quasi-polygonal ferrite, and Widmanstätten ferrite according to the grain boundary shape. Meanwhile, Krauss and Thompson [17] named the ferritic microstructure in low-carbon/ultra-low-carbon steel based on their previous research results. Similar to the results of the ISIJ Bainite Research Group, ferrite is polygonal (or equiaxed) ferrite according to the grain boundary shape and transformation temperature, Widmanstätten ferrite, and quasi-polygonal (or massive) ferrite were named, and the low-temperature transformation were largely classified into bainitic (or acicular) ferrite and granular (or granular bainitic) ferrite according to their shape. Koo et al. [18] classified and named the low-temperature transformed into granular bainite, degenerate upper bainite, lath martensite, and lower bainite according to the shape of ferrite, the presence or absence of secondary phases, and arrangement, unlike the microstructures reported by existing researchers. If the ferrite and low-temperature transformation phase that are commonly distinguished by several researchers are summarized, they can be broadly classified into polygonal ferrite, quasipolygonal ferrite, granular bainitic ferrite, bainitic ferrite, and martensite. Therefore, the microstructure of this paper was largely classified into bainitic ferrite, martensite, pearlite, and Widmanstätten ferrite, and acicular-shaped ferrite that was not completely transformed from prior austenite was classified as acicular ferrite.

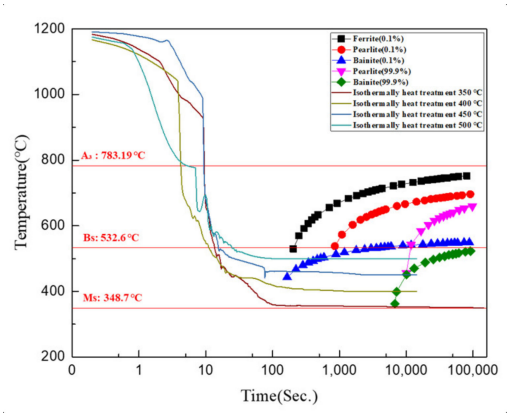


Figure 2. The temperature of the specimen measured during isothermal heat treatment based on the CCT curve calculated with Jmatpro was substituted.

Figure 3 shows the results of microstructural analysis using optical microscopy. The phases were distinguished by the colors resulting from LePera etching. Typically for the LePera etching method [19,20], ferrite is blue/green, bainite and pearlite are brown, and martensite is white. The classification of bainitic ferrite and perlite was judged using SEM images. As shown in Figure 3a, the microstructure of the as-cast sample isothermally heat treated at 350 °C mainly consisted of bainitic ferrite (BF), with a small portion of acicular ferrite (AF) and martensite (M). Similarly, Figure 3b,c show the microstructures after heat treatment at 400 and 450 °C, respectively, in which BF, AF, and M can be observed. However, for the sample isothermally heat treated at 500 °C (Figure 3d), Widmanstätten ferrite (WF) and pearlite (P) were observed, which is consistent with the data reported by Bramfitt and Speer [15].

In contrast, the hot-rolled samples exhibited somewhat different results. As shown in Figure 4, unlike the as-cast steel, the microstructure of hot-rolled sample isothermally heat treated at 350 °C comprised almost BF and a small amount of AF. After annealing at 400 °C (Figure 4b), AF was observed in addition to BF, the same as at 350 °C. As shown in Figure 4c, the hot-rolled sample isothermally heat treated at 450 °C contained BF, AF, and M, similar to that in the cast steel heat treated at this temperature. In addition, for the sample heat treated at 500 °C (Figure 4d), WF and P were observed. After isothermal heat treatment, the microstructures of cast steel and hot-rolled steel were analyzed at low

magnification on the surface, middle, and center. As a result, various phases are generally uniformly distributed.

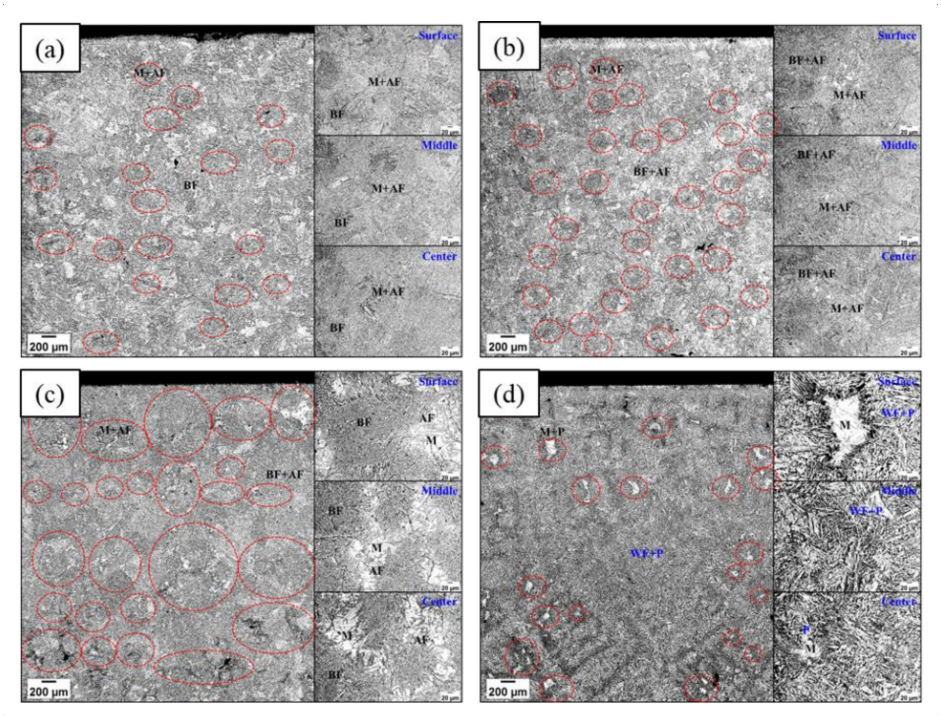


Figure 3. Microstructures of medium-carbon low-alloy steel isothermally heat treated for 240 min: cast steel heat treated at (**a**) 350 °C, (**b**) 400 °C, (**c**) 450 °C, and (**d**) 500 °C.

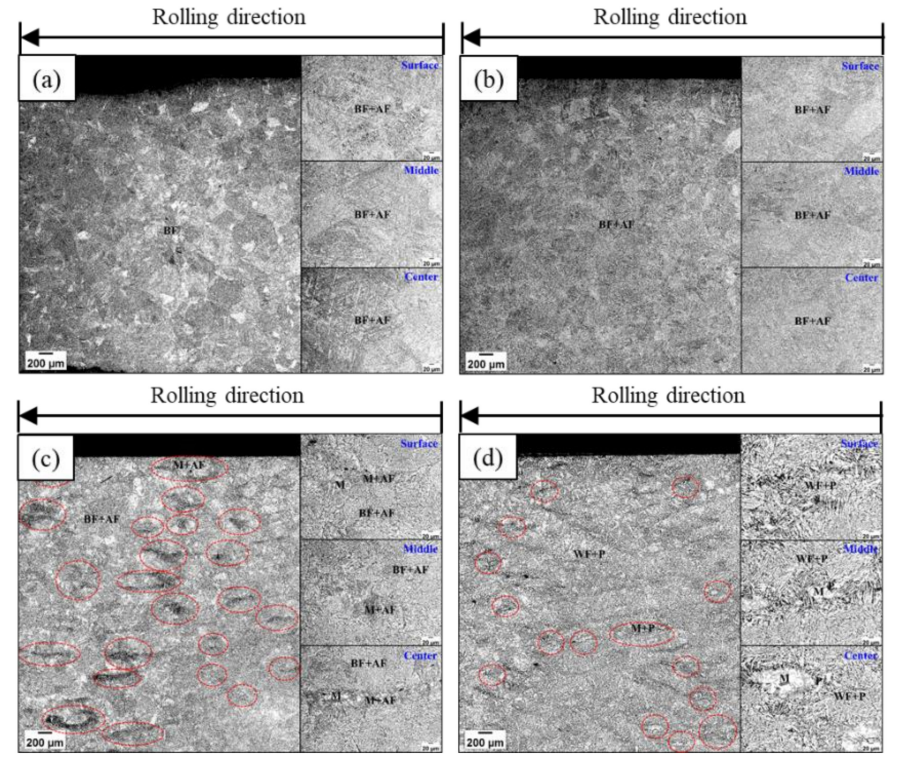


Figure 4. Microstructures of medium-carbon low-alloy steel isothermally heat treated for 240 min: hot-rolled steel heat treated at (**a**) 350 °C, (**b**) 400 °C, (**c**) 450 °C, and (**d**) 500 °C.

It has long been known that the lower bainite does not form in medium-carbon steels with a carbon content of less than 0.4 wt% [21]. During isothermal heat treatment of the 0.3 wt% carbon sample, mostly upper bainite formed rather than lower bainite. According to the EBSD analysis, the austenite phase fraction was less than 2%. Based on these results, it appears that there was almost no retained austenite. The reduction in the size and fraction of retained austenite due to the reduction in the carbon content is thought to be related to the redistribution of carbon to austenite resulting from the formation of BF. This indicates that if the carbon content of the alloy decreases, it is very unlikely that carbon will redistribute to the austenite phase; rather, it will mostly reside in BF. For this reason, when the carbon content of the alloy is low, a higher fraction of BF is formed before the carbon content of the retained austenite reaches a level at which BF formation is thermodynamically difficult owing to shear transformation. Therefore, when the carbon content is low, the BF phase fraction increases, and the retained austenite phase fraction and grain size decrease [22,23].

Figures 5 and 6 shows the SEM analysis of the bainitic ferrite phase under isothermal heat-treatment conditions. BF is typically composed of cementite and dislocation-rich BF. The high dislocation concentration of BF increases its hardness. Cementite in bainitic ferrite does not typically exhibit a parallel arrangement or plate form but appears as many irregularly arranged precipitates inside small dislocation-rich ferrite grains.

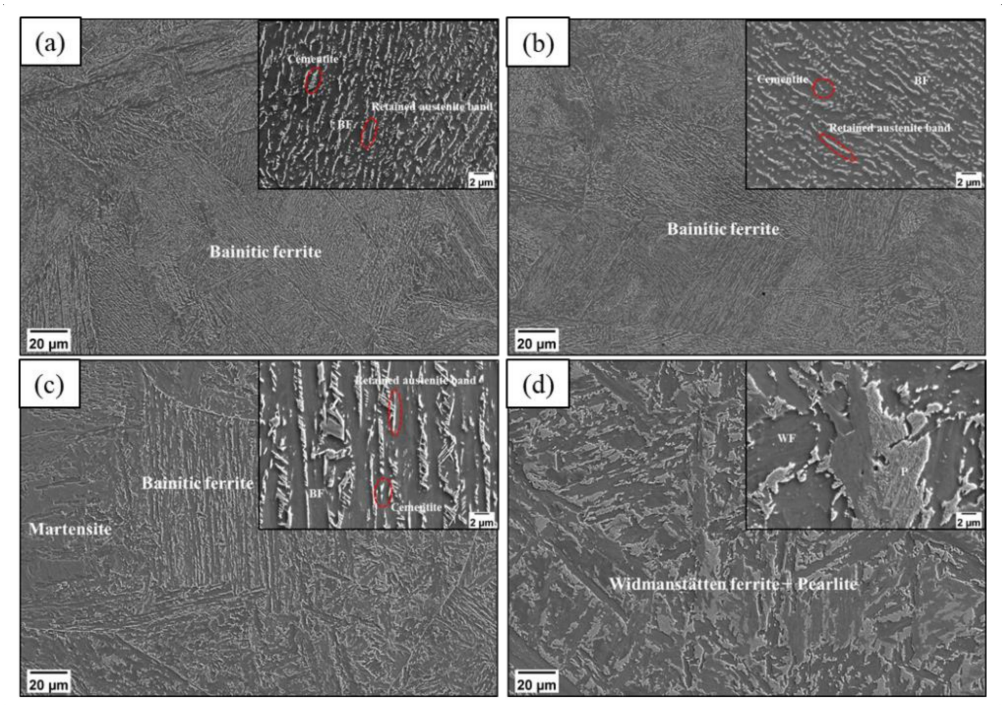


Figure 5. SEM micrographs of medium-carbon low-alloy steel isothermally heat treated for 240 min: cast steel heat treated at (**a**) 350 °C, (**b**) 400 °C, (**c**) 450 °C, and (**d**) 500 °C.

Based on the Koo et al. [18], Figures 5 and 6 appear to show mostly degenerated upper bainite. In addition, according to Yin et al., the degenerated upper bainite forms in three stages. The first stage is the formation of the primary ferrite plate, the second stage is the thickening of the ferrite plate, and the last stage is the deformation of the retained austenite band, which is initiated from the cementite [24]. In particular, the second stage occurs through the precipitation of cementite from austenite containing excess carbon from the primary ferritic plates. Thus, cementite can precipitate, and more ferrite forms as the carbon content decreases [25,26]. As shown in Figures 5 and 6, the size and distribution of BF and cementite after isothermal heat treatment at 350 and 400 °C were similar. When the isothermal heat-treatment temperature was 450 °C, the BF and cementite sizes rapidly increased. The observed coarsening of ferrite is considered to be caused by coalescence

and subsequent diffusive growth [10,27]. As previously stated, coarse WF and P formed (Figures 3 and 4) when the isothermal heat-treatment temperature was 500 °C. This type of phase formation is related to the sympathetic nucleation mechanism of rod-shaped or lath-shaped ferrite subunits [28–30].

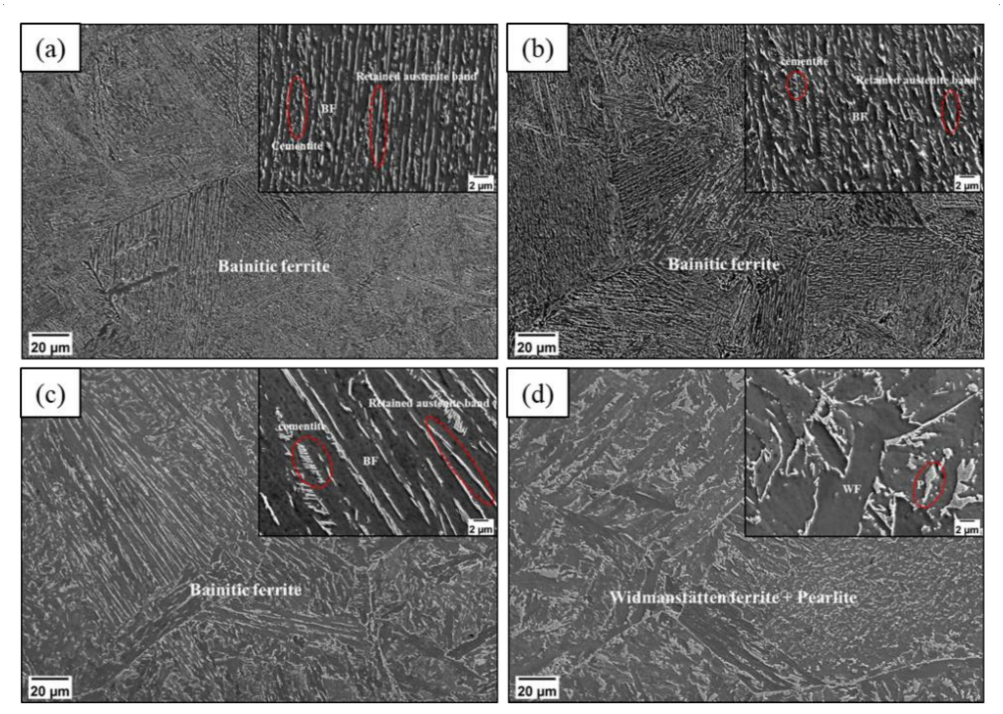


Figure 6. SEM micrographs of medium-carbon low-alloy steel isothermally heat treated for 240 min: hot-rolled steel heat treated at (**a**) 350 °C, (**b**) 400 °C, (**c**) 450 °C, and (**d**) 500 °C.

The phase fraction was measured by analyzing Figures 3 and 4 using an image analysis program. Using an optical micrograph after LePera etching, the phases can be easily distinguished by their color: white (M), brown (BF and P), and blue (AF). Figure 7 shows the measured phase fractions of the cast steel and hot-rolled steel after isothermal heat treatment. For the cast steel, the BF phase fraction decreased, and the AF phase fraction increased as the isothermal heat-treatment temperature increased from 350 to 450 °C. The M phase fraction was similar at 350 and 400 °C but increased sharply at 450 °C. WF and P appeared at 500 °C, and WF was dominant. For the hot-rolled steel, the BF phase fraction decreased as the isothermal heat-treatment temperature increased from 350 to 450 °C, which is the same behavior as that of the cast steel. However, at 350 °C, the AF fraction decreased sharply, unlike cast steel. Additionally, the M fraction was hardly found. The AF phase fraction increased as the isothermal heat-treatment temperature increased from 400 and 450 °C. Similar to the cast steel, the M phase fraction increased rapidly at 450 °C, and WF and P appeared at 500 °C. In summary, BF, AF, and M were found in the cast steel heat treated at 350 °C, but only AF, BF was found in the hot-rolled steel. At 400 °C, same as 350 °C, BF and AF were observed in both specimens, but M was observed only in cast steel. In the hot-rolled steel, the BF phase fraction was somewhat higher than that of the cast steel, and the AF phase fractions were relatively low. At 450 °C, the BF phase fraction was higher in the hot-rolled steel than that of the cast steel, and the AF and M phase fractions were lower. At 500 °C, the WF phase fraction was higher in the hot-rolled steel than that of the cast steel, and even though some P was found, the P phase fraction was relatively small. Based on these results, the hot-rolled steel was almost transformed into bainitic ferrite after isothermal heat treatment at 350 °C for 240 min. For the other heat-treatment conditions, a complete bainitic ferrite phase transformation was

not achieved. In particular, for isothermal heat treatment at 500 °C, the cooling rate was sufficiently low that WF and P formed regardless of the additional hot deformation process.

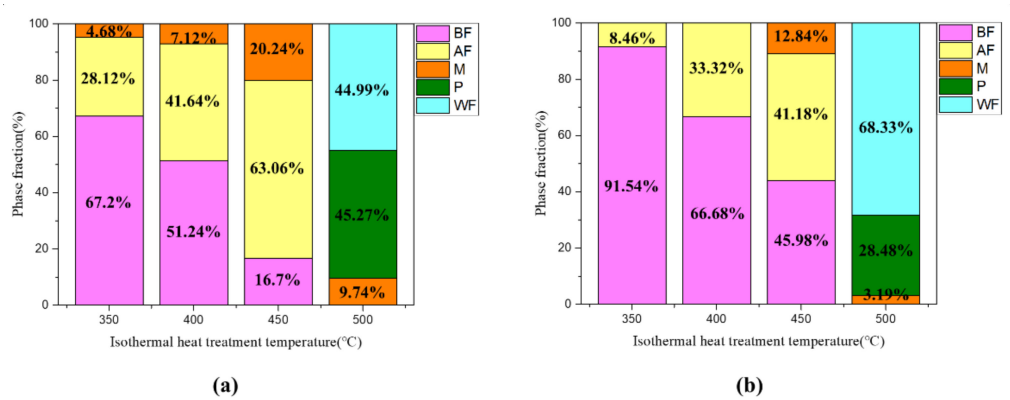


Figure 7. Phase fractions of (**a**) cast and (**b**) hot-rolled medium-carbon low-alloy steel after isothermal heat treatment.

Because grain boundary features directly affect the mechanical properties of the alloy, the crystal orientation distribution was measured using EBSD. Based on this analysis, the effective size of grains with a misorientation of 15° or higher was a major factor. The microstructure formed by shear transformation exhibits a hierarchical structure consisting of prior austenite grains and packets, blocks, and laths. Among them, interfaces with a misorientation of 15° or higher correspond to the interfaces surrounding prior austenite grains or packets and blocks. Therefore, the effective grain size was evaluated based on both the prior austenite grain boundaries and the interfaces surrounding the packets and blocks [31]. Figure 8 quantifies the dependence of the grain size on the heat-treatment temperature of the cast and hot-rolled steel. For the cast steel, the grain size decreased as the isothermal heat-treatment temperature increased from 350 to 500 °C, although it did not change significantly between 450 and 500 °C. However, for the hot-rolled samples, the grain size was similar at 350 and 400 °C, but it decreased as the temperature increased to 450 °C. When the temperature increased to 500 °C, the grain size increased dramatically. This is related to the phase fractions after isothermal heat treatment (Figure 7). As the isothermal heat-treatment temperature of the cast steel increased from 350 to 450 °C, the AF and M phase fractions both increased, and the grain size decreased accordingly. Then, the grain size decreased rapidly when the M phase fraction increased at 450 °C. At 500 °C, the grain size was reduced owing to the increase in the P and M phase fractions. In the hot-rolled steel, the AF phase fraction increased from 8.46% to 33.32% as the temperature increased to 400 from 350 °C, where the BF phase fraction was 91.54%, but AF did not significantly contribute to the grain size because the grain size was similar. In contrast, as the temperature increased to 450 °C, the grain size decreased owing to the increase in the M phase fraction. However, as the temperature increased to 500 °C, the grain size rapidly increased owing to the decrease in the P and M phase fractions. Comparing the cast and hot-rolled steels, hot deformation decreased the grain size for heat treatments between 350 °C and 400 °C, but the grain size was similar at 450 °C due to the difference in the M phase fraction. As the temperature increased to 500 °C, the grain size of the hot-rolled steel increased rapidly owing to the lower P and M phase fractions compared with those in the cast steel. Therefore, at this isothermal heat-treatment condition, the P and M phases contribute significantly to the overall grain size.

The kernel average misorientation (KAM) is an index used to indirectly evaluate dislocation density [32]. The KAM value generally decreases as the dislocation density decreases, and conversely, increases as the dislocation density increases. As the rolling rate increases, the crystal orientation behavior within a single grain changes. This phenomenon occurs regardless of the presence or absence of an inhomogeneous carbide band, and the difference in crystal orientation can be quantified using the KAM. The KAM map plots

the average value of the difference between the crystal orientation of one measurement point and the crystal orientations of adjacent measurement points, and it can be used to visualize the local change in the amount of residual strain. Generally, a higher KAM value (red color) corresponds to a higher M phase fraction [33,34].

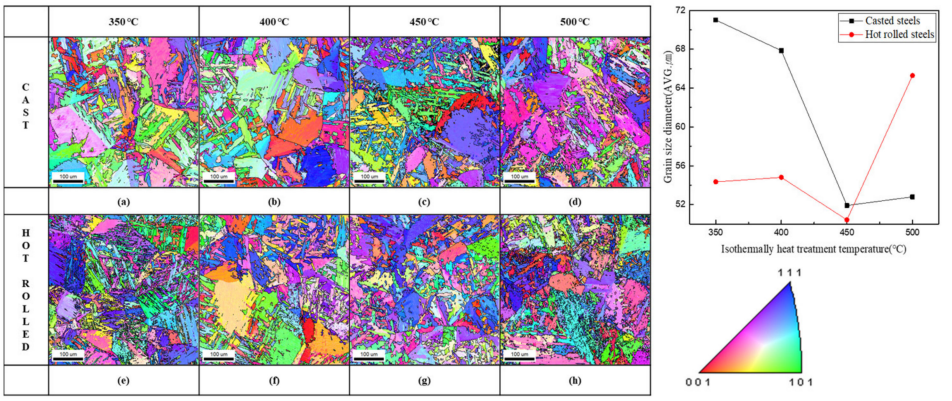


Figure 8. EBSD orientation maps and grain sizes of medium-carbon low-alloy steel isothermally heat treated for 240 min: cast steel heat treated at (**a**) 350 °C, (**b**) 400 °C, (**c**) 450 °C, and (**d**) 500 °C and hot-rolled steel heat treated at (**e**) 350 °C, (**f**) 400 °C, (**g**) 450 °C, and (**h**) 500 °C.

High KAM values in yellow-green, excluding red, indirectly indicate the dislocation density due to strain. As shown in Figure 9 KAM maps, the cast steel had a similar dislocation density distribution at 350 and 400 °C. However, as the temperature increased to 450 °C, a high dislocation density was observed, and a red region caused by M was also identified. This is because the M phase fraction was high at 450 °C. At 500 °C, a lower dislocation density was observed. The change in the distribution of dislocation density with the heat-treatment temperature of the hot-rolled steel was similar to that of the cast steel, but the dislocation density was higher. In line with this, it has been shown that numerous carbon clusters exist in BF, which is related to the low solubility of carbon atoms in the body-centered cubic (BCC) matrix. This is also the reason the carbon clusters in BCC-structured BF tend to pin dislocations and interfere with the slip behavior. This leads to strain concentration around the carbon clusters, resulting in high KAM values [35–37].

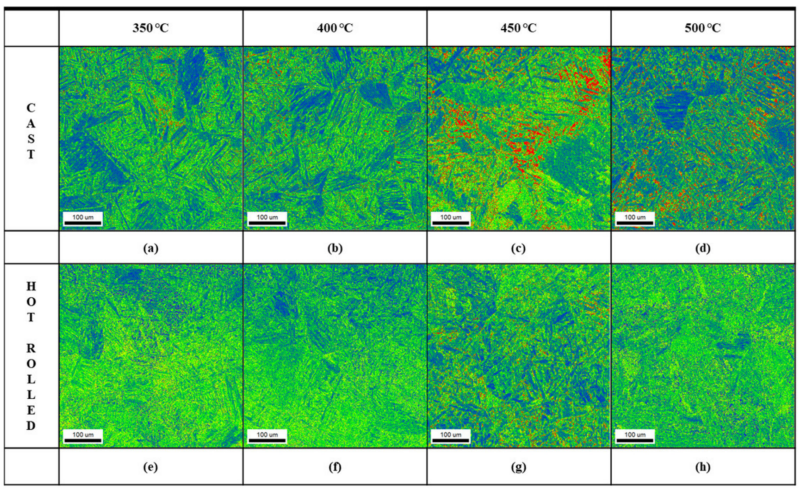


Figure 9. EBSD KAM maps of medium-carbon low-alloy steel isothermally heat treated for 240 min: cast steel heat treated at (**a**) 350 °C, (**b**) 400 °C, (**c**) 450 °C, and (**d**) 500 °C and hot-rolled steel heat treated at (**e**) 350 °C, (**f**) 400 °C, (**g**) 450 °C, (**h**) and 500 °C.

3.2. Mechanical Properties

The mechanical properties, which depend on casting defects and grain size, were investigated along with microstructural changes in the cast and hot-deformed medium-carbon steels. As shown in Figure 10, the hardness of both the cast steel decreased as the isothermal heat-treatment temperature increased from 350 to 500 °C. As can be seen from the microstructure investigation, as the isothermal treatment temperature increased, the phase fraction of hard phases (BF and M) decreased and soft phases (AF and WF) increased. Hot-rolled steel has the highest hardness at 350 °C because the hard phase (BF) occupies most of it. However, as the temperature increased to 400 °C, the soft phase (AF) increased and the hardness decreased sharply. As the temperature increases to 450 °C, the soft phase (AF) increases, but the hardness is similar to 400 °C due to M. At 500 °C, the soft phase (WF) increased and martensite(M) decreased, and the hardness decreased compared to 450 °C. In summary, various hardness appears depending on the fraction of hard phase (BF and M) and soft phase (AF and WF). Additionally, M contributes the most to hardness.

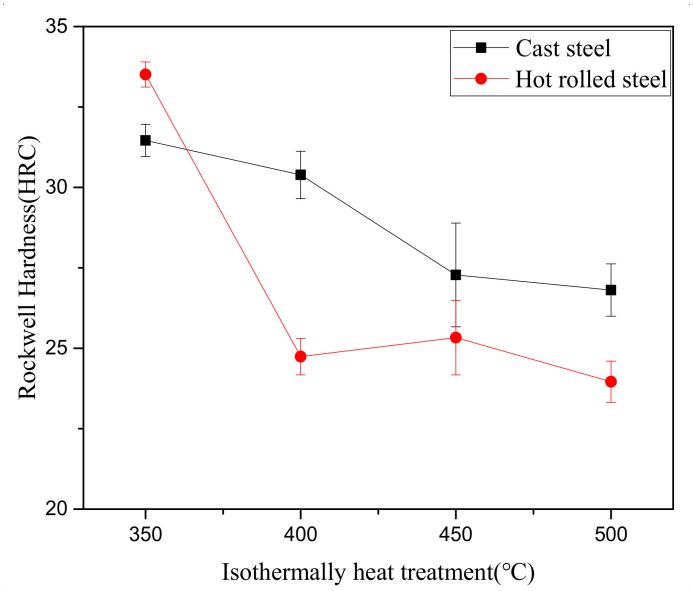


Figure 10. Variation in the hardness of medium-carbon low-alloy steel with the isothermal heat-treatment temperature.

Figure 10 shows the stress–strain behavior for the various heat-treatment conditions. During phase transformations (such as BF or M), the dislocation density increases rapidly, which results in the presence of some dislocations even in annealed microstructures [38,39]. The high yield strength should be related to the presence of M in the microstructure. The diffusion of carbon from the growing bainitic ferrite plate also enriches the surrounding austenite, thus increasing its stability, until the reaction stops completely. As a result, the undeformed prior austenite regions can transform into M [29,40].

Figures 11 and 12 show the tensile tests results for the various isothermal heat-treatment conditions. As a result of the tensile tests measurement, the yield strength and tensile strength decreased as the overall isothermal heat-treatment temperature increased from 350 to 500 °C, which is consistent with the aforementioned hardness measurement values. As the cast steel increased from 350 to 400 °C, the M and AF fraction increased, resulting in a slight decrease in yield and tensile strength. At 450 °C, the fraction of M increased, but the strength decreased sharply because the fraction of AF accounted for most. At 500 °C, compared with 450 °C, the M fraction decreased and the strength decreased. In contrast, the hot-rolled steel under the same heat-treatment conditions showed slight differences. The highest yield and tensile strength were shown at 350 °C, where the BF fraction was highest. However, as the temperature increased to 400 °C, the fraction of soft AF increased, and the yield and tensile strength decreased rapidly. With the increase

of 450 °C, the yield strength slightly increased from 400 °C due to the M phase, but the tensile strength decreased slightly. At 500 °C, the yield and tensile strength decreased as the fraction of soft WF increased while the fraction of M decreased.

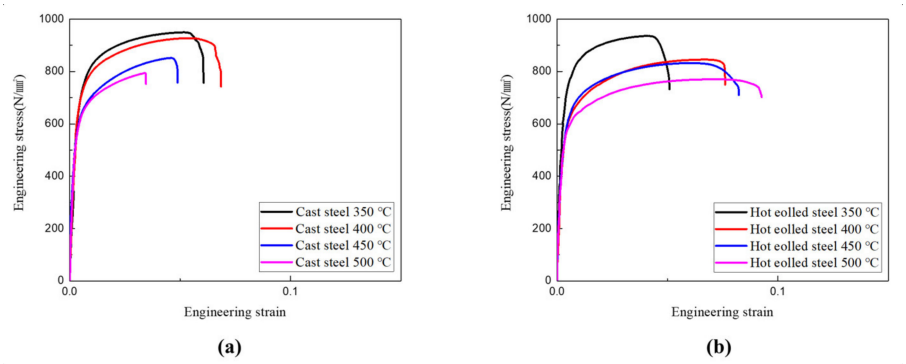


Figure 11. Strain–stress curves of (**a**) cast and (**b**) hot-rolled medium-carbon low-alloy steel after isothermal heat treatment.

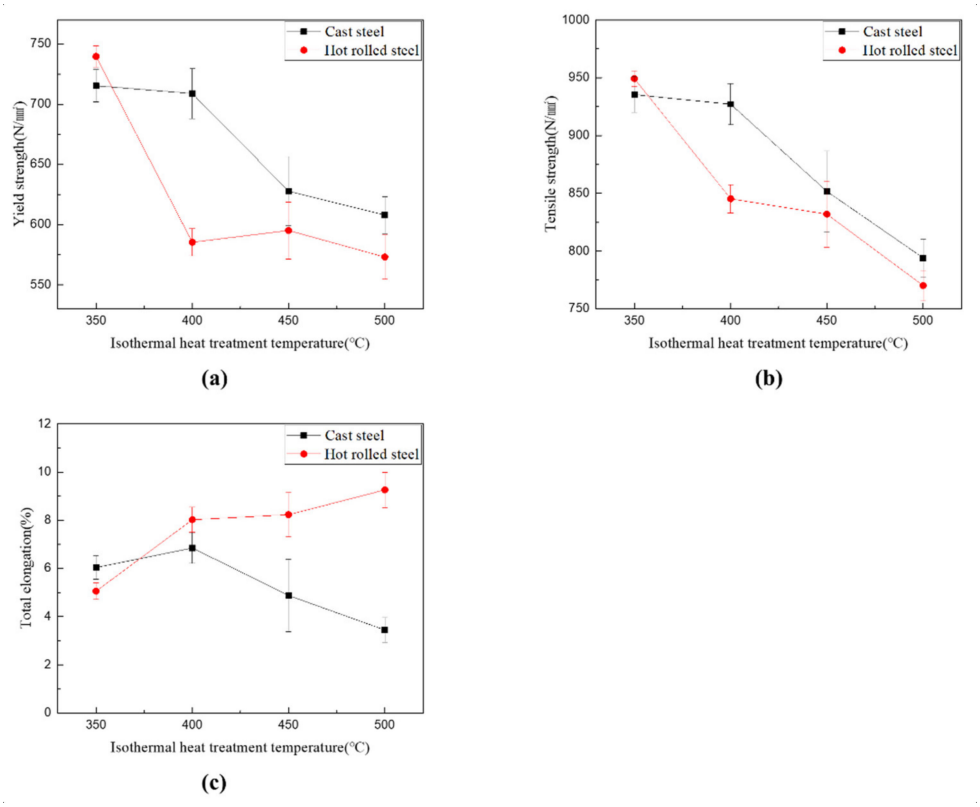


Figure 12. Variation in the (**a**) Yield strength, (**b**) Tensile strength and (**c**) elongation of medium-carbon low-alloy steel with the isothermal heat-treatment temperature.

As the isothermal heat-treatment temperature decreases, the cooling rate increases, and carbon supersaturation in BF also increases as the cooling rate increases. This increase in carbon supersaturation distorts the lattice of BF, which impedes dislocation movement; thus, the tensile strength and hardness increased, but the elongation decreased [41]. However, unlike cast steel, the elongation generally increased as the isothermal heat-treatment temperature increased. This difference in ductility is undoubtedly correlated with the reduction in casting defects and the differences in the phase fractions. Because the difference in the M phase fraction was high, the elongation differed. Therefore, various phases are

transformed according to the isothermal treatment temperature. These various phases act in combination to affect microstructure and mechanical properties.

4. Conclusions

The microstructure and mechanical properties analysis after isothermal heat treatment of medium-carbon low-alloy steel showed the following results.

1. There was a difference in the phase transformation and phase fraction of cast steel and hot-rolled medium-carbon low-alloy steel during isothermal heat treatment at 350~500 °C for 240 min. The cast and hot-rolled steel were not completely transformed into bainitic ferrite.
2. When the isothermal heat-treatment temperature decreased, the bainitic ferrite phase became more prevalent, but the opposite behavior was observed for acicular ferrite. Austenite which did not transform into bainitic ferrite during isothermal heat treatment mostly transformed into martensite.
3. When the isothermal heat-treatment temperature was 500 °C, the major phases were Widmanstätten ferrite and pearlite in both the cast and hot-rolled steels.
4. The average grain size of cast steel decreases rapidly from 350 to 450 °C; and at 500 °C, it is similar to 450 °C. Hot-rolled steel decreases moderately from 350 to 450 °C but increases rapidly at 500 °C. The yield strength of the cast and hot-rolled steel decreases as the isothermal heat-treatment temperature increases. The yield strength of cast steel decreases rapidly as it increases from 400 to 450 °C, and the yield strength of hot-rolled steel decreases rapidly as it increases from 350 to 400 °C. Hardness showed a similar trend to yield strength. At each isothermal heat-treatment temperature, mechanical properties depend on complex factors such as phase fractions, and grain size.
5. The highest strength and hardness were exhibited at the isothermal heat-treatment temperature of 350 °C, which was similar to the Ms temperature.

Author Contributions: Conceptualization, B.S.; methodology, B.S.; software, B.S; validation, S.Y., K.K. and S.C.; formal analysis, K.K.; investigation, B.S.; writing—review and editing, S.H.; supervision, S.H.; All authors have read and agreed to the published version of the manuscript.

Funding: This research received no external funding.

Institutional Review Board Statement: Not applicable.

Informed Consent Statement: Not applicable.

Data Availability Statement: Data available on request from the authors.

Acknowledgments: This research was supported by the Ministry of Trade, Industry, and Energy (MOTIE) in Korea under the Fostering Global Talents for Innovative Growth Program (P0008750) supervised by the Korea Institute for Advancement of Technology (KIAT).

Conflicts of Interest: The authors declare no conflict of interest.

References

1. Ståhlkrantz, A.; Hedström, P.; Sarius, N.; Sundberg, H.; Kahl, S.; Thuvander, M.; Borgenstam, A. Effect of Tempering on the Bainitic Microstructure Evolution Correlated with the Hardness in a Low-Alloy Medium-Carbon Steel. *Metall. Mater. Trans. A* **2020**, *51A*, 6470–6481. [CrossRef]
2. Podder, A.S. Tempering of a mixture of bainite and retained austenite. Ph.D. Thesis, University of Cambridge, Cambridge, UK, 2011.
3. Peet, M.J. Transformation and tempering of low-temperature bainite. Ph.D. Thesis, University of Cambridge, Cambridge, UK, 2010.
4. Peet, M.J.; Babu, S.S.; Miller, M.K.; Bhadeshia, H. Tempering of low-temperature bainite. *Metall. Mater. Trans. A* **2017**, *48A*, 3410–3418. [CrossRef]
5. He, S.; He, B.; Zhu, K.; Huang, M. On the correlation among dislocation density, lath thickness and yield stress of bainite. *Acta Mater.* **2017**, *135*, 382–389. [CrossRef]

6. Garcia-Mateo, C.; Peet, M.; Caballero, F.; Bhadeshia, H. Tempering of hard mixture of bainitic ferrite and austenite. *Mater. Sci. Technol.* **2004**, *20*, 814–818. [CrossRef]
7. Garcia-Mateo, C.; Caballero, F. Ultra-high-strength bainitic steels. *ISIJ Int.* **2005**, *45*, 1736–1740. [CrossRef]
8. Steven, W.; Haynes, A.G.J. The temperature of formation of martensite and bainite in low alloy steels, some effects of chemical composition. *J. Iron Steel Inst.* **1956**, *183*, 349.
9. Krauss, G. Deformation and fracture in martensitic carbon steels tempered at low temperatures. *Metall. Mater. Trans. B* **2001**, *32*, 205–221. [CrossRef]
10. Bhadeshia, H.K.D.H. *Bainite in Steels: Transformation, Microstructure and Properties*, 2nd ed.; IOM Communications Ltd: London, UK, 2001.
11. Tomita, Y. Effect of martensite morphology on mechanical properties of low alloy steels having mixed structure of martensite and lower bainite. *Mater. Sci. Technol.* **1991**, *7*, 299–306. [CrossRef]
12. Tomita, Y.; Okabayashi, K. Mechanical properties of 0.40 pct C-Ni-Cr-Mo high strength steel having a mixed structure of martensite and bainite. *Metall. Trans. A* **1985**, *16*, 73–82. [CrossRef]
13. Rao, T.V.L.N.; Dikshit, S.N.; Malakondaiah, G.; Rao, P.R. On mixed upper bainite-martensite in an AISI 4330 steel exhibiting an uncommonly improved strength-toughness combination. *Scr. Metall. Mater.* **1990**, *24*, 1323–1328. [CrossRef]
14. Kirkaldy, J.S. Prediction of microstructure and hardenability in low alloy steels. In Proceedings of the International Conference on Phase Transformation in Ferrous Alloys, Philadelphia, PA, USA, 4–6 October 1983; AIME: Warrendale, PA, USA, 1983; pp. 125–148.
15. Bramfitt, B.L.; Speer, J.G. A perspective on the morphology of bainite. *Metall. Trans. A* **1990**, *21*, 817. [CrossRef]
16. Araki, T.; Kozasu, I.; Tankechi, H.; Shibata, K.; Enomoto, M.; Tamehiro, H. *Atlas for Bainitic Microstructures, Continuous-Cooled Zw Microstructures of Low-Carbon Steel*; ISIJ: Tokyo, Japan, 1992; Volume 1, pp. 4–5.
17. Krauss, G.; Thompson, S.W. Ferritic microstructures in continuously cooled low-and ultralow-carbon steels. *ISIJ* **1995**, *35*, 937. [CrossRef]
18. Koo, J.Y.; Luton, M.J.; Bangaru, N.V.; Petkovic, R.A.; Fairchild, D.P.; Petersen, C.W.; Asahi, H.; Hara, T.; Terada, Y.; Sugiyama, M.; et al. Metallurgical design of ultra-high strength steels for gas pipelines. In *Proceedings of the Thirteenth International Offshore and Polar Engineering Conference*; ISOPE: Honolulu, HI, USA, 2003; p. 10.
19. LePera, F.S. Improved etching technique for the determination of percent martensite in high-strength dual-phase steels. *Metallography* **1979**, *12*, 263. [CrossRef]
20. Zakerinia, H.; Kermanpur, A.; Najafizadeh, A. Color metallography; a suitable method for characterization of martensite and bainite in multiphase steels. *ISSI* **2009**, *6*, 14.
21. Ohmori, Y.; Honeycombe, R.W.K. The isothermal transformation of plain carbon austenite. *Suppl. Trans. ISIJ* **1971**, *11*, 1160–1164.
22. Quidort, D.; Bréchet, Y. The role of carbon on the kinetics of bainite transformation in steels. *Scr. Mater.* **2002**, *47*, 151. [CrossRef]
23. Quidort, D.; Brechet, Y.J. A model of isothermal and non isothermal transformation kinetics of bainite in 0.5% C steels. *ISIJ Int.* **2002**, *42*, 1010. [CrossRef]
24. Yin, J.; Hillert, M.; Borgenstam, A. Morphology of upper and lower bainite with 0.7 mass pct C. *Metall. Mater. Trans. A* **2017**, *48A*, 4006–4024. [CrossRef]
25. Sandvik, B.P.J. The bainite reaction in Fe-Si-C alloys: The secondary stage. *Metall. Trans. A* **1982**, *13A*, 789–800. [CrossRef]
26. Tsuzaki, K.; Kodai, A.; Maki, T. Formation mechanism of bainitic ferrite in an Fe-2 Pct Si-0.6 Pct C alloy. *Metall. Mater. Trans. A* **1994**, *25A*, 2009–2016. [CrossRef]
27. Okaguchi, S.; Ohtani, H.; Ohmori, Y. Morphology of Widmanstätten and bainitic ferrites. *Mater. Trans.* **1991**, *32*, 697–704. [CrossRef]
28. Aaronson, H.I.; Spanos, G.; Masamura, R.A.; Vardiman, R.G.; Moon, D.W.; Menon, E.S.K.; Hall, M.G. Sympathetic nucleation: An overview. *Mater. Sci. Eng. B* **1995**, *32*, 107–123. [CrossRef]
29. Aaronson, H.I.; Reynolds, W.T.; Purdy, G.R. The incomplete transformation phenomenon in steel. *Metall. Mater. Trans. A* **2006**, *37*, 1731–1745. [CrossRef]
30. Wu, K.M.; Enomoto, M. Three-dimensional morphology of degenerate ferrite in an Fe–C–Mo alloy. *Scr. Mater.* **2002**, *46*, 569–574. [CrossRef]
31. Lee, E.H.; Yu, C.J.; Lee, H.B.; Kim, J.H.; Suh, D.W. Influence of Si and Al contents and isothermal treatment condition on the microstructure and tensile properties in ultra-high strength Fe-0.2C-2.0Mn martensite-bainite complex phase steels. *Korean J. Met. Mater.* **2021**, *59*, 602–612. [CrossRef]
32. Wright, S.I.; Nowell, M.M.; Field, D.P. A review of strain analysis using electron backscatter diffraction. *Microsc. Microanal.* **2011**, *17*, 316–329. [CrossRef]
33. Lee, J.M.; Lee, S.I.; Lim, H.S.; Hwang, B. Effect of Isothermal Heat Treatment on the Microstructure and Mechanical Properties of Medium-Carbon Bainitic Steels. *Korean J. Mater. Res.* **2018**, *28*, 522. [CrossRef]
34. Kim, J.S.; Kim, J.N.; Kang, C.Y. Effect of Thermo-mechanical Treatment on the Formation Behavior of Martensite in 316L Stainless Steel. *Korean J. Met. Mater.* **2018**, *56*, 265.
35. Kang, J.; Zhang, F.; Long, X.; Lv, B. Low cycle fatigue behavior in a medium-carbon carbide-free bainitic steel. *Mater. Sci. Eng. A* **2016**, *666*, 88–93. [CrossRef]

36. Sourmail, T.; Smanio, V. Low temperature kinetics of bainite formation in high carbon steels. *Acta Mater.* **2013**, *61*, 2639–2648. [CrossRef]
37. Timokhina, I.B.; Beladi, H.; Xiong, X.; Adachi, Y.; Hodgson, P.D. Nano scale microstructural characterization of a nanobainitic steel. *Acta Mater.* **2011**, *59*, 5511–5522. [CrossRef]
38. Chen, C.T.; Lei, T.S. The processing window for austempering ductile iron. *Mater. Tran. JIM* **1999**, *40*, 82–85. [CrossRef]
39. Sandvik, B.P.J.; Wayman, C.M. Characteristics of lath martensite: Part I. Crystallographic and substructural features. *Metall. Trans. A* **1983**, *14*, 809. [CrossRef]
40. Hatem, T.M.; Zikry, M.A. A model for determining initial dislocation-densities associated with martensitic transformations. *Mater. Sci. Technol.* **2011**, *27*, 1570. [CrossRef]
41. Madariaga, I.; Romero, J.L.; Gutierrez, I. Upper acicular ferrite formation in a medium-carbon micro alloyed steel by isothermal transformation: Nucleation enhance-ment by CuS. *Metall. Mater. Trans. A* **1998**, *29*, 1003–1115. [CrossRef]